Available online at www.sciencedirect.com
SCIENCE DIRECT®
Atmospheric Environment 39 (2005) 575–586
ATMOSPHERIC ENVIRONMENT
www.elsevier.com/locate/atmosenv

The dependence of tropospheric ozone production rate on ozone precursors ☆

Lawrence I. Kleinman

Atmospheric Sciences Division, Brookhaven National Laboratory, Upton, NY 11973, USA

Received 12 April 2004; accepted 19 August 2004

Abstract

An analytic formula is derived expressing the tropospheric O_3 production rate, $P(O_3)$, as a power law function of radical production rate, NO_x concentration, and VOC–OH reactivity. Power law exponents depend on a single parameter, L_N/Q, which is the fraction of free radicals removed by reactions with NO_x. The formula reproduces the functional form of $P(O_3)$ obtained from photochemical box model calculations. Ozone production rates are shown to have a smooth transition between previously derived low and high NO_x limits. Potential applications of this formula include analysis of day to day and place to place variations in $P(O_3)$, with $P(O_3)$ either obtained from measurements collected during field campaigns or produced as output from chemical-transport models.
Published by Elsevier Ltd.

Keywords: Ozone production rate; Tropospheric photochemistry; Ozone sensitivity; Low and high NO_x; Ozone precursors

1. Introduction

A now standard exercise in most comprehensive photochemistry field campaigns is to use observed chemical concentrations to calculate a chemical rate of O_3 production, $P(O_3)$. There are 3 ways of proceeding. $P(O_3)$ can be determined as the rate of reaction of peroxy radicals with NO based on measured NO and peroxy radicals (e.g. Cantrell et al., 1996; Penkett et al., 1999; Mihelcic et al., 2003), $P(O_3)$ can be calculated from a photochemical model that is constrained by observed concentrations of non-radical species (e.g. Frost et al., 1998; Jaeglé et al., 2001; Kleinman et al., 2002a), and $P(O_3)$ can be determined from the photostationary state relations (e.g. Ridley et al., 1992; Volz-Thomas et al., 2003), albeit with problems. The comparison of $P(O_3)$'s calculated in these ways is an active area of research and provides a stringent test of our understanding of tropospheric O_3 photochemistry. $P(O_3)$ is also of interest for determining the chemical component of O_3 tendency in different regions (e.g. Liu et al., 1992; Jacob et al., 1996; Cantrell et al., 2003). The dependence of $P(O_3)$ on O_3 precursors provides information of the O_3 forming process in regions where O_3 is a pollutant with health and other environmental impacts (e.g. Daum et al., 2000a, b, 2003; Dommen et al., 2002; Thornton et al., 2002; Kleinman et al., 2002a).

In order to understand why $P(O_3)$ varies from time to time and place to place it is desirable to have simple, transparent formulas that show how $P(O_3)$ depends on

 This research was performed under the auspices of the United States Department of Energy under Contract No. DE-AC02-98CH10886

1352-2310/$ - see front matter Published by Elsevier Ltd.
doi:10.1016/j.atmosenv.2004.08.047

its precursors. For the limiting cases in which NO_x concentration is very high or very low such formulas already exist and have been used to interpret data from field campaigns (e.g. Kleinman et al., 1994; Carpenter et al., 1997, 2000; Daum et al., 2000a, b; Dommen et al., 2002). Formulas valid for mid-NO_x conditions have been derived for the simplified case of a CO/CH_4 atmosphere (Carpenter et al., 2000). In this article we derive a general relation between $P(O_3)$ and the concentration of the atmospheric reactants responsible for its production. These reactants can be divided into 3 somewhat overlapping categories, NO_x, VOCs, and radical precursors. Our result will be a formula which gives the power law dependence of $P(O_3)$ on NO_x concentration, VOC reactivity, and radical production rate. This formula depends on a single quantity, L_N/Q, where L_N is the rate of radical removal by reactions with NO_x and Q is the rate of radical production. L_N/Q is therefore the fraction of free radicals removed from the atmosphere by reaction with NO_x, the remaining fraction being removed by combination reactions between free radicals.

While NO_x concentration, VOC–OH reactivity, and radical production rate are quantities that can be directly related to commonly made observations, L_N/Q is a parameter with less intuitive appeal. It is not an independent precursor variable in the same sense as NO_x concentration, VOC reactivity, and radical production rate; it can be described in terms of those 3 variables (Kleinman et al., 2001). Instead it is a dependent variable that conveys information on where an air parcel is in the continuum of states ranging from the high NO_x regime characteristic of polluted conditions to the low NO_x regime characteristic of rural or remote regions. Under normal circumstances a polluted air mass evolves from a high NO_x state with L_N/Q near 1 to a low NO_x state with L_N/Q near 0 due to chemical oxidation of VOCs and NO_x and due to dilution with cleaner background air. It is known that the evolution of an airmass from a high NO_x state to a low NO_x state is accompanied by a transition between VOC sensitive O_3 chemistry to NO_x sensitive O_3 chemistry. Because the dominant end product of photochemistry changes from NO_x oxidation species such as HNO_3 to radical combination species such as peroxides during this transition, the ratio of these 2 compounds can be used as an indicator of NO_x and VOC limited photochemistry (Sillman, 1995; Tonnesen and Dennis, 2000a, b; Hammer et al., 2002; Martilli et al., 2002; Sillman and He, 2002; Thielmann et al., 2002). Low and high NO_x states also provide a framework for discussing the dynamical behavior of tropospheric photochemistry, including multiple steady states, limit cycles, and chaos (Stewart, 1995; Field et al., 2001).

Our objective in this article is to present and evaluate a general formula that shows how $P(O_3)$ depends on its precursors. This work builds on an earlier study (Kleinman et al., 1997) in which the sensitivity of $P(O_3)$ to NO_x concentration and VOC reactivity was derived. Here we add an additional equation that shows the sensitivity of $P(O_3)$ to radical production rate. It is then straight-forward to obtain a formula that shows the power law dependence of $P(O_3)$ on NO_x, VOC reactivity, and radical production rate. Our discussion of the $P(O_3)$ formula focuses on the governing photochemical reactions and the approximations made in the derivation including the assumption that PAN is in steady state.

Evaluation of the $P(O_3)$ formula is done using a combination of observed and predicted quantities. NO_x concentration, VOC reactivity, and radical production rate are determined from observed concentrations, solar irradiance, and published rate constants. A box model with species concentrations constrained to observed values (Kleinman et al., 2002a, b) is used to calculate $P(O_3)$ and L_N/Q. A test of the approximate power law formula is a determination of whether or not calculated $P(O_3)$ has the predicted functional form. The power law formula succeeds in quantitatively reproducing most of the model results. However, we offer this formula only as a qualitative tool to understand $P(O_3)$ variations as our analysis does not address questions of model completeness or accuracy in the same way that a closure experiment would.

2. Theory

Qualitative formulas for $P(O_3)$ have been derived elsewhere for the limiting low and high NO_x cases (Kleinman et al., 1994; Daum et al., 2000a, b). In this section we extend the derivation to show the dependence of $P(O_3)$ on radical production rate, NO_x concentration, and VOC reactivity for cases intermediate between the low and high NO_x limits.

2.1. $P(O_3)$ formula

Derivations are based on the usual photochemical equations (e.g. Seinfeld and Pandis, 1997), a subset of which are repeated below. Equations are divided into 3 categories representing the initiation, cycling, and termination steps in the overall O_3 forming chain reaction.

Initiation:

R1 $O_3 + h\nu \rightarrow O^1D$

$O^1D + H_2O \rightarrow 2\,OH$

R2 $HCHO + h\nu \rightarrow 2\,HO_2$

R3 $Alkene + O_3 \rightarrow radicals$

Chain Propagation or Cycling:

R4 $OH + VOC_i \rightarrow a\,HO_2 + b\,RO_2 + c\,RCO_3$
R5 $HO_2 + NO \rightarrow NO_2 + OH$
R6 $RO_2 + NO \rightarrow d\,(NO \rightarrow NO_2\ \text{conversions}) + \text{HC oxidation products}$
R7 $RCO_3 + NO \rightarrow e\,(NO \rightarrow NO_2\ \text{conversions}) + \text{HC oxidation products}$
R8 $NO_2 + h\nu \rightarrow NO + O$
$O + O_2 \rightarrow O_3$

Termination:

radical + NO_x

R9 $OH + NO_2 \rightarrow HNO_3$
R10 $RO_2 + NO \rightarrow$ organic nitrate
R11a $CH_3CO_3 + NO_2 \rightarrow PAN$
R11b $PAN \rightarrow CH_3CO_3 + NO_2$

radical + radical

R12 $HO_2 + HO_2 \rightarrow H_2O_2$
R13 $RO_2 + HO_2 \rightarrow ROOH$
R14 $OH + HO_2 \rightarrow H_2O + O_2$
R15 $RO_2 + R'O_2 \rightarrow$ products

Photolysis and ozonolysis reactions split chemical bonds, forming free radicals that initiate photochemical O_3 production. R1 and R2 in that order are usually the most important initiation reaction. The sum total radical production rate will be denoted as Q.

Chain propagation is a cyclic pathway in which OH oxidizes VOCs (R4) forming peroxy radicals which convert NO to NO_2 (R5–R7) which is photolyzed forming O_3 (R8). R6 and R7 are multi-step reactions in which peroxy radicals are regenerated leading to more than one NO to NO_2 conversion (Atkinson, 2000). The cycle is completed by regenerating OH in R5 and NO in R8. In R4 and the following text, VOC_i could be a hydrocarbon, CO, an oxygenated compound such as HCHO, or any other species that reacts with OH producing peroxy radicals. The OH reactivity of a mixture of VOCs is given by,

$$VOC_R = \Sigma k_i[VOC_i], \quad (1)$$

where the k's are rate constants for reaction with OH. Although VOC reactivity and radical production are treated as independent variables in the production of O_3, these 2 precursor categories overlap as compounds such as HCHO contribute to both. R4 is written to allow for the production of 3 types of peroxy radicals, not all of which would be produced from any single VOC. The total number of NO to NO_2 conversions caused by the peroxy radicals formed in R4 assuming that they all react with NO as in R5–R7 is given by

$$Y_i = a + bd + ce. \quad (2)$$

Ozone production stops with the chain termination reactions in which radicals are destroyed. Conservation of radicals requires that the rate of termination equal the rate of initiation. There are two families of termination reactions in which free radicals either react with NO_x or with each other. An important parameter describing O_3 photochemistry is the fraction of radicals removed in each pathway. For this purpose we use L_N/Q where L_N is the rate of removal by reactions of the radical + NO_x type. Formation of PAN removes radicals in R11a while PAN dissociation is a radical source in R11b. We will use the symbol $P(PAN)$ to indicate the net PAN production rate given as the rate of R11a minus R11b. Otherwise, the symbol "P" will stand for a chemical production rate and not include loss processes.

The derivation of formulas for $P(O_3)$ depends on several assumptions. In the low NO_x case defined by $L_N/Q \rightarrow 0$, the rate limiting step is taken to be reaction of peroxy radical with NO (R5–R7). It is assumed that radical loss by peroxide formation is equal to radical production, yielding

$$P(O_3) = k_t/(2k_{eff})^{1/2} Q^{1/2}[NO], \quad (3)$$

where k_t is a composite rate constant for R5–R7 and k_{eff} describes the effective rate of peroxide formation (Kleinman et al., 1994). Under high NO_x conditions, $L_N/Q \rightarrow 1$ and $P(O_3)$ is given by

$$P(O_3) = Q\Sigma Y_i k_i[VOC_i]/k_9[NO_2] \quad (4)$$

(Daum et al., 2000a, b). The major assumptions used to derive (4) are that the reaction of OH with VOCs (R4) are rate limiting (Sillman, 1995),

$$P(O_3) \approx \Sigma Y_i k_i[OH][VOC_i] \quad (5)$$

that radical + radical reactions (R12–R15) can be ignored, and that the reaction of OH with NO_2 (R9) is the predominant radical sink:

$$L_N \approx P(HNO_3) = k_9[OH][NO_2]. \quad (6)$$

A general formula for $P(O_3)$ valid at intermediate NO_x concentration is based on equations for the relative sensitivity of $P(O_3)$ to its precursors.

The sensitivity to NO_x and VOCs is given in Kleinman et al. (1997):

$$\frac{d\ln P(O_3)}{d\ln[NO_x]} = \frac{(1-3/2\,L_N/Q)}{(1-1/2\,L_N/Q)}, \quad (7)$$

$$\frac{d\ln P(O_3)}{d\ln(VOC_R)} = \frac{1/2\,L_N/Q}{(1-1/2\,L_N/Q)}. \quad (8)$$

Eqs. (7) and (8) express sensitivities in terms of logarithmic derivatives, i.e. $d\ln P/d\ln X = (X/P)\,dP/DX$, with the property that $d\ln P/d\ln X = 1$ when a (small) n% change in X produces an n% change in P. Eq. (7) is written with NO_x as the independent variable rather than NO as originally derived. In deriving (7) we had assumed that NO and NO_2 are proportional, an approximation that is discussed in a following section. In the Appendix we derive an analogous expression for the sensitivity of $P(O_3)$ to radical production rate:

$$d\ln P(O_3)/d\ln Q = (1/2)/(1-1/2\,L_N/Q). \quad (9)$$

The derivation of (9) in the Appendix closely follows that used to obtain (7) and (8) and serves to illustrate the approximations made in arriving at those equations.

We obtain our desired formula by writing $P(O_3)$ as:

$$P(O_3) = KQ^{C1}[NO_x]^{C2}(VOC_R)^{C3}, \quad (10)$$

where, for a particular choice of L_N/Q; K, $C1$, $C2$, and $C3$ are constants. Eq. (10) provides a local fit to $P(O_3)$, strictly speaking valid only at a particular value of L_N/Q, but in practice useable over a range of values. A similar formalism was used by Jaeglé et al. (2001) to determine the power law dependence of $P(O_3)$ in the upper troposphere on Q and NO_x. Differentiating (10) with respect to Q, NO_x, or VOCs yields, respectively,

$$d\ln P(O_3)/d\ln Q = C1, \quad (11)$$

$$d\ln P(O_3)/d\ln[NO_x] = C2, \quad (12)$$

$$d\ln P(O_3)/d\ln(VOC_R) = C3. \quad (13)$$

The exponents $C1$, $C2$, and $C3$ depend only on L_N/Q and are given by (7)–(9). Eq. (10) gives the functional dependence of $P(O_3)$ on O_3 precursors but falls short of providing a complete analytic formula for $P(O_3)$ because the dependence of K on L_N/Q has not been evaluated.

A graph of $C1$, $C2$, and $C3$ as a function of L_N/Q is shown in Fig. 1. As indicated in Table 1, $C1$, $C2$, and $C3$ have the limiting low and high NO_x values given in (3) and (4), respectively. At $L_N/Q = 1/2$, the NO_x and VOC curves cross indicating an equal sensitivity of $P(O_3)$ to both precursors. The NO_x sensitivity curve has a zero crossing at $L_N/Q = 2/3$. At this point $P(O_3)$ has a maximum value with respect to changes in NO_x concentration. An analogous feature appearing in ozone isopleth plots is the O_3 ridge line (e.g. Seinfeld and Pandis, Fig. 5.15, 1997).

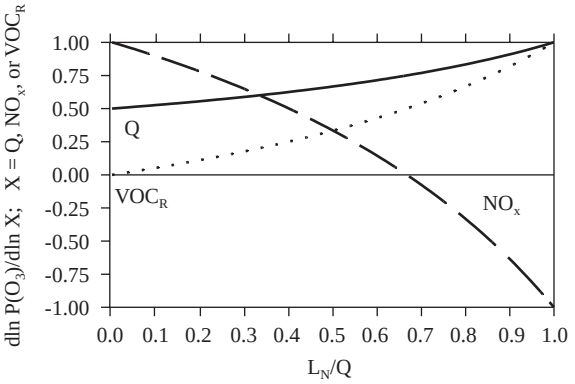

Fig. 1. Relative sensitivity of $P(O_3)$ to radical production rate, Q; NO_x concentration; and VOC reactivity, VOC_R, as a function of the fraction of radicals removed by reaction with NO_x, L_N/Q. Curves are from (7)–(9).

Table 1
Dependence of $P(O_3)$ on Q, NO_x, and VOC_R

L_N/Q	Exponents for $P(O_3) = K\,Q^{C1}\,[NO_x]^{C2}\,(VOC_R)^{C3}$		
	$C1$	$C2$	$C3$
0.0	0.5	1.0	0.0
0.5	0.67	0.33	0.33
0.67	0.75	0.0	0.5
1.0	1.0	−1.0	1.0

2.2. NO or NO_2?

In the derivation of (7)–(9) it is assumed that NO and NO_2 are proportional, an approximation which can be improved upon. NO_x enters the derivation of the sensitivity equations in 2 places. In (A1), $P(O_3)$ is given by the rate of reaction of peroxy radicals with NO and in (A7) L_N is given by the rate of reaction of OH with NO_2. The limiting low and high NO_x formulas for $P(O_3)$, (3) and (4), show that this dual dependence on NO and NO_2 reduces to a dependence on NO at low NO_x and a dependence on NO_2 at high NO_x. This feature can be incorporated in (10) by using NO as an independent variable at low L_N/Q and NO_2 at high L_N/Q. In a following section we empirically determine the values of L_N/Q which give better results with NO or NO_2 as an independent variable.

2.3. PAN

PAN and analogous compounds are temporary reservoirs for NO_x. Formation of reservoir compounds removes NO_x and free radicals in one location, almost all of which is put back into the atmosphere at another

location when theses compounds dissociate. As discussed in Kleinman et al. (2002b), PAN and analogous compounds have not been included in our calculations on the assumption that these species are in steady state. Under steady state conditions the rate of formation of PAN is equal to the rate of dissociation and PAN is then neither a source or sink of free radicals. Although we expect this to be true on average, most of our studies have been done close to emission sources in air masses that have an active photochemistry, where we expect PAN to be a net radical sink. Our ability to improve upon the steady state PAN approximation has been limited by the absence of PAN measurements in our data sets.

The effect of PAN on $P(O_3)$ sensitivities has been addressed by Sillman (1995), Spirig et al. (2002), and Sillman and He (2002). Sillman (1995) noted that the point at which $P(O_3)$ has an equal sensitivity to NO_x and VOC occurs when

$$P(HNO_3) = 2\,P(\text{Peroxide}) \tag{14}$$

i.e., where the number of radicals removed by forming HNO_3 is equal to the number removed by forming peroxides. Fig. 1 and Table 1, derived under the assumption that PAN is in steady state, indicate that equal sensitivity to NO_x and VOC occurs at $L_N/Q = 1/2$, a result that reduces to Sillman's formula when formation of organic nitrates and PAN is ignored (when $L_N = P(HNO_3)$). In deriving (14), Sillman assumed that PAN and O_3 production rates are proportional. Using the same approximation, equations in Kleinman et al. (1997) describing effects of organic nitrates show that the sensitivity of $P(O_3)$ to NO_x and VOCs is given by

$$\frac{d\ln P(O_3)}{d\ln[NO_x]} = \frac{(1 - 3/2\,L_N/Q + 1/2\,P(PAN)/Q)}{(1 - 1/2\,L_N/Q)}, \tag{15}$$

$$\frac{d\ln P(O_3)}{d\ln(VOC_R)} = \frac{(1/2\,L_N/Q - 1/2\,P(PAN)/Q)}{(1 - 1/2\,L_N/Q)}. \tag{16}$$

Equating the right-hand sides of (15) and (16) to determine the point at which NO_x and VOC sensitivity are equal yields (14) after a change in notation. Applying the same approximation to $d\ln P(O_3)/d\ln Q$ does not change (9). Eq. (10) still applies except that $C2$ and $C3$ are given by the right-hand sides of (15) and (16) instead of (7) and (8).

For positive values of $P(PAN)$, (15) and (16) show that NO_x sensitivity is increased and VOC sensitivity reduced, relative to the no—PAN case. Spirig et al. (2002) have a numerical example of this effect in a case with high PAN concentrations ($PAN \approx HNO_3 \approx 10$ ppb). They find that a calculation without PAN overpredicts VOC sensitivity, relative to a calculation that includes PAN, in regions where PAN is forming, and overpredicts NO_x sensitivity in regions where PAN is dissociating. A comparison of Figs. 16a and b in Spirig et al., shows these over and underpredictions cause a 1 h shift in a transition between VOC and NO_x sensitive photochemistry but do not change the qualitative sense of the calculations.

2.4. L_N/Q

According to (7)–(10) the functional form of $P(O_3)$ Is determined entirely by L_N/Q. In this section we show how L_N/Q depends on O_3 precursors. We rely on formulas given in Kleinman et al. (2001), with a change in notation whereby ω takes the place of α. Using the same approximations that were employed in deriving the $P(O_3)$ sensitivity equations (see Appendix), L_N/Q is given by the solution of a quadratic equation:

$$L_N/Q = -\omega/2 + (\omega^2 + 4\omega)^{1/2}/2, \tag{17}$$

where

$$\omega = (k_9[NO_2]k_5\gamma[NO]/(VOC_R))^2(1/(2\,Qk_{eff})), \tag{18}$$

$$\gamma = [HO_2]/([HO_2] + [RO_2]). \tag{19}$$

In a following section we will show the relation between L_N/Q and NO_x for 2 cities, Phoenix and Houston. Here we note a few qualitative features. Eqs. (17)–(19) depend on the HO_2 to total peroxy radical ratio through γ and k_{eff}. However, that dependence is weak and a reasonable guess for the split between HO_2 and RO_2 will usually suffice. If we assume that NO and NO_2 are proportional, then L_N/Q is a monotonic function of $NO_x^4/(VOC_R)^2\,(1/Q)$. Because NO_x appears to the fourth power in this expression, NO_x concentration more than any other variable determines L_N/Q.

3. Model

A constrained steady state (CSS) box model is used to calculate $P(O_3)$ and L_N/Q. This is the same model used in previous studies in which aircraft observations in Nashville, New York City, Phoenix, Philadelphia, and Houston were used to determine O_3 production rates in those cities (Kleinman et al., 2002a). Inputs to the CSS model include the chemical species; O_3, NO, CO, speciated hydrocarbons, HCHO, H_2O_2, organic peroxides, SO_2, and water vapor; actinic flux approximated from a UV measuring Eppley radiometer (Madronich, 1987); temperature; and pressure. Organic nitrate formation is included in the CSS calculations but PAN and analogous compounds are assumed to be in steady state and are not included as calculated or constrained variables. Calculations are based on the RADM2 chemical mechanism (Stockwell et al., 1990) for anthropogenic pollutants and the mechanism of Paulson and Seinfeld (1992) for isoprene oxidation. Observed concentrations of approximately 100 VOCs are parsed

into RADM2 categories according to structure and reactivity.

The CSS calculations yield the concentrations of OH, HO_2, RO_2s and NO_2 which are in steady state with the observed mixture of stable atmospheric species. The model keeps track of the rates of all individual reactions. $P(O_3)$ is determined as the rate for conversion of NO to NO_2 by peroxy radicals which is the sum of R5, R6, and R7. L_N is the rate of radical loss due to R9 and R10, Q is the rate of radical production due to all photolysis reactions (2 of which are R1 and R2) plus the rate due to ozonolysis reactions, R3.

4. Experimental

Chemical concentrations and other input parameters for the CSS calculations are taken from aircraft observations made during the course of 5 field campaigns in Nashville, New York City, Phoenix, Philadelphia, and Houston. VOC observations determined by canister samples are generally the limiting factor in assembling the input data to a CSS calculations. For each VOC sample, other trace gasses and parameters are averaged over the sample time period (about 30 s). Experimental techniques and data sets have been previously described (Kleinman et al., 2002a, b; Daum et al., 2003 and references therein).

A few general features of the 5 city data set should be noted. Samples used in this study are all taken during daylight hours. Most samples are at mid-boundary layer height. About 5% are in much cleaner air above the boundary layer. There is a wide variation in chemical concentrations and physical conditions, some of which has been explored in previous articles and some of which will be the topic of a future study comparing O_3 production in the 5 cities. Among the distinctive features are very high VOC reactivity in Houston, a very dry atmosphere and low radical production rate in Phoenix, high isoprene concentrations in Nashville, and high NO_x concentrations in power plant plumes. Although our objective in this study is not to describe the 5 cities, it is important to note that the conditions under which sampling was done and $P(O_3)$ calculated are wide ranging. Thus the evaluation of (10) is likewise done for a diverse range of conditions.

5. L_N/Q for 2 Cities

The dependence of L_N/Q on NO_x was illustrated in Kleinman et al. (2001) using photochemical calculations based on aircraft data collected in Phoenix, AZ (see also Carmichael et al. (2003) for an application to East Asia and the Pacific Ocean). Fig. 2a for the Phoenix data set shows an almost one to one correspondence between

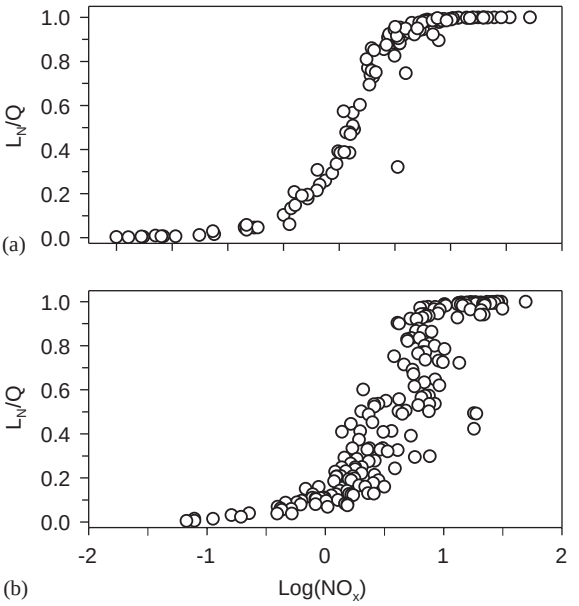

Fig. 2. The dependence of L_N/Q on log of NO_x concentration in (a) Phoenix and (b) Houston. Each point represents a sampling location where a CSS calculation was done yielding a value for L_N/Q.

L_N/Q and NO_x. For Phoenix we find that high NO_x conditions ($L_N/Q > 0.9$, $P(O_3)$ given by (4)) apply whenever NO_x is greater than 3 ppb. Low NO_x conditions ($L_N/Q < 0.1$, $P(O_3)$ given by (3)) apply whenever NO_x is lower than 0.3 ppb.

Fig. 2b shows a similar plot of L_N/Q vs. NO_x based on aircraft data collected in Houston, TX. Compared with Phoenix, points are shifted to higher NO_x concentration and there is much more scatter. Of the 5 cities that we have studied, Phoenix and Houston represent 2 extremes. In Phoenix, emissions are dominated by mobile sources yielding a narrow range of ambient NO_x to VOC_R ratios. Houston has a more diverse emissions mixture which on average has a NO_x to VOC_R ratio lower than Phoenix. It is still possible to pick out low and high NO_x conditions in Houston based on NO_x concentration, but quantifying the middle range without a detailed calculation or evaluation of (17)–(19) is problematic.

6. Formula evaluation

Our objective is to test Eq. (10). To do so we will compare values of $P(O_3)$ obtained from a CSS box model with those determined from $Q^{C1}[\mathrm{NO\ or\ NO_2}]^{C2}(\mathrm{VOC}_R)^{C3}$, which within a proportionality constant is equal to $P(O_3)$. Q, [NO or NO_2], and VOC_R are determined from rate constant data and observed

concentrations, temperature, and UV solar irradiance. A CSS model calculation, based on the same set of observations, is used to calculate L_N/Q which according to (7)–(9) determines the exponents $C1$, $C2$, and $C3$ appearing in the power law formula for $P(O_3)$. Our evaluation procedure has to take into account the fact that the proportionality constant, K, in (10) depends on L_N/Q and is not a priori determined.

There are 624 CSS data points available for evaluating (10). City by city totals are 92 from Nashville, 79 from NYC, 123 from Phoenix, 138 from Philadelphia, and 192 from Houston. The data set has been divided into 10 subsets in which L_N/Q varies from 0 to 1 in increments of 0.1. The first subset has L_N/Q between 0 and 0.1, the second between 0.1 and 0.2, etc. As a way of stressing the wide range of conditions represented by the calculations, Table 2 shows the minimum, maximum, and median values of $P(O_3)$ for each L_N/Q subset. Lowest values of $P(O_3)$ have L_N/Q in the range 0–0.1 or 0.9–1.0. The lowest decile of L_N/Q contains samples with very clean air from the boundary layer and free troposphere, some of which are calculated to have net O_3 destruction after taking into account O_3 chemical loss processes. The highest L_N/Q decile is mainly composed of samples with high NO_x concentrations, in a few instances more than 50 ppb due to power plant plumes. Photochemical production of O_3 is then greatly diminished because radical concentrations are reduced by reaction of OH with NO_2. Highest values of $P(O_3)$ are from Houston (Kleinman et al., 2002a) and occur at intermediate values of L_N/Q.

For each subset we plot the CSS value of $P(O_3)$ versus Q^{C1} [NO or NO_2]^{C2} $(VOC_R)^{C3}$. Values of $C1$, $C2$, and $C3$ are determined for the midpoint of each L_N/Q interval according to (7)–(9). As K is not predicted beforehand, we are testing the functional form of (10), not whether it gets the right value for $P(O_3)$. By construction, K has zero first derivatives and is therefore nearly constant over a small range of L_N/Q. Thus we expect that our test plots will yield straight lines. Fig. 3 contains 10 panels which show plots of $P(O_3)$ versus Q^{C1} [NO or NO_2]^{C2} $(VOC_R)^{C3}$ for the 10 data subsets defined by L_N/Q. Each panel has 2 plots, one using NO and one using NO_2 as the independent variable. A linear least squares regression has been done for the 20 plots yielding the straight line fits shown in Fig. 3. Results are summarized in Table 2. Correlation coefficients show that for L_N/Q between 0 and 0.7, (10) is best evaluated using NO; for $L_N/Q \geqslant 0.7$, NO_2 gives a higher r^2. NO and NO_2 perform about the same for L_N/Q in the range 0.6–0.7, as the power law expression predicts zero dependence on NO_x at $L_N/Q = 2/3$. Allowing for a switch in independent variable from NO to NO_2 at $L_N/Q = 0.7$, the power law formula explains 96–99% of the variability in $P(O_3)$. Fig. 3 shows that our formula does equally well in reproducing the CSS results for both low and high $P(O_3)$ cases. As Table 2 indicates, the average percent error in predicting how $P(O_3)$ responds to Q, NO_x, and VOC_R varies from 9% to 13% depending on L_N/Q subset. Table 2 also shows results for splitting L_N/Q into 4 subsets, one apiece for low and high NO_x conditions and 2 for mid-NO_x conditions.

Table 2
Characteristics of CSS calculated $P(O_3)$ and comparison with $P(O_3)$ power law formula

L_N/Q	# samples	$P(O_3)$ (ppb h^{-1})			Linear least squares[a]: r^2		% Error[b]	K[c]
		Min.	Max.	Median	NO	NO_2		
0.0–0.1	136	0.04	12	2.7	0.96	0.75	15	22
0.1–0.2	92	0.7	20	6.5	0.97	0.69	9	16
0.2–0.3	61	1.4	71	8.4	0.98	0.86	13	12
0.3–0.4	35	1.9	22	11	0.97	0.72	9	8.5
0.4–0.5	25	2.0	155	13	0.99	0.97	11	7.1
0.5–0.6	29	1.9	46	15	0.96	0.89	12	4.5
0.6–0.7	16	3.0	46	17	0.96	0.95	12	3.5
0.7–0.8	32	2.9	67	22	0.97	0.99	10	3.8
0.8–0.9	34	2.5	32	15	0.89	0.98	9	4.8
0.9–1.0	164	0.6	61	7.4	0.87	0.99	9	6.4
0.0–0.3	289	0.04	20	4.5	0.99		12	16
0.3–0.5	60	1.9	155	12	0.99		13	8.1
0.5–0.7	45	1.9	46	16	0.95		13	3.9
0.7–1.0	230	0.6	67	9.0		0.98	13	4.5

[a]From linear regression forced through origin: CSS $P(O_3)$ versus Q^{C1} [NO or NO_2]^{C2} $(VOC_R)^{C3}$.
[b]100 × Standard error of $P(O_3)$ estimate/Average $P(O_3)$. NO used for $L_N/Q = 0-0.7$, NO_2 for $L_N/Q > 0.7$.
[c]Slope of regression line when $P(O_3)$ = ppb h^{-1}, Q = ppb h^{-1}, NO_x = ppb, and VOC_R = s^{-1}. NO used for $L_N/Q = 0-0.7$, NO_2 for $L_N/Q > 0.7$.

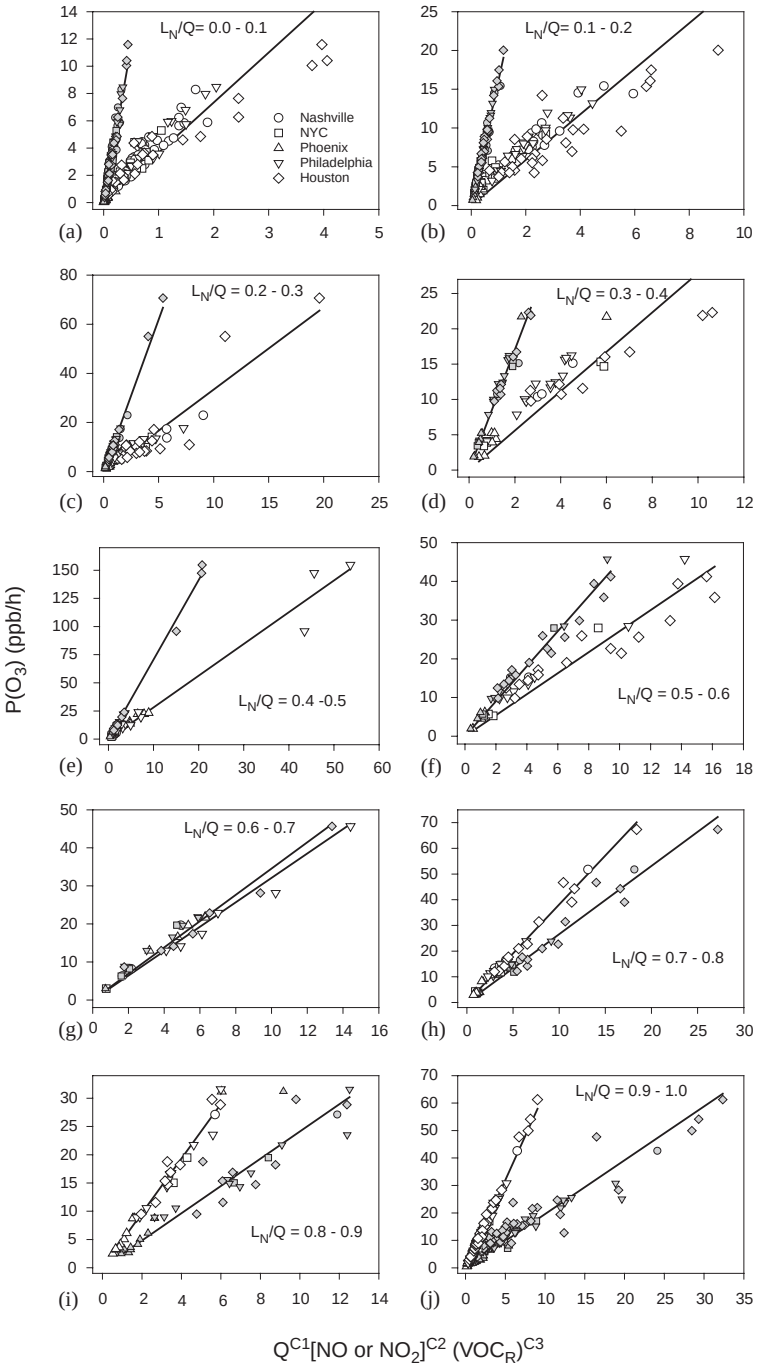

Fig. 3. Calculated values of $P(O_3)$ from a CSS box model versus power law formula for $P(O_3)$. The CSS calculations have been divided into 10 subsets in which L_N/Q varies from 0 to 1 in increments of 0.1 as indicated on the 10 panels. In each panel the power law expression for $P(O_3)$, Q^{C1} [NO or NO_2]^{C2} (VOC_R)^{C3}, is evaluated using NO (shaded symbols) and NO_2 (open symbols). $C1$, $C2$, and $C3$, are determined from (7) to (9) using the midpoint of the L_N/Q range. Straight lines are linear least squares fit to data points forced through origin. The squared correlation coefficients, r^2, are given in Table 2. Symbols shown in the first panel identify points as based on data collected in Nashville, TN; New York City, NY; Phoenix, AZ; Philadelphia, PA, or Houston, TX.

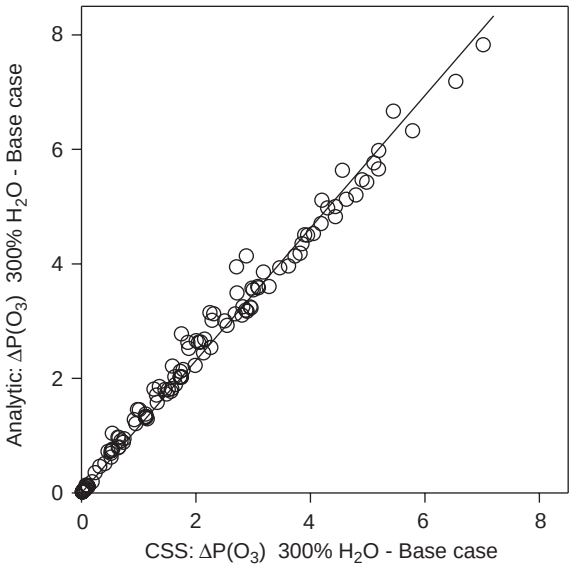

Fig. 4. Test of analytic formula, Eq. (10), for the dependence of $P(O_3)$ on Q. Each axis gives the increase in $P(O_3)$, $\Delta P(O_3)$, caused by a tripling of water vapor concentration in the Phoenix calculations. The ordinate is calculated from the CSS model and the abscissa calculated from Eq. (20). The analytic formula uses the base case values of L_N/Q and $P(O_3)$. Straight line is a linear least square regression fit, passing though the origin with a slope of 1.16.

Eq. (10) still succeeds in providing semi-quantitative predictions of how $P(O_3)$ varies with precursors. In all cases, (10) is evaluated using an L_N/Q at the center of the interval. Choosing an L_N/Q from outside the appropriate range is equivalent to trying to fit the data set with the wrong formula, which is reflected in a significant increase in the percent error (not shown in Table or Figures).

Eq. (10) was derived using relative sensitivities that give the response of $P(O_3)$ to small changes in NO_x, VOC_R, and Q (7)–(9). For that reason neither (10) or the plots in Fig. 3 should be used to infer the change in $P(O_3)$ due to large changes in O_3 precursors. Large changes are accompanied by a change in L_N/Q which in essence shifts the system from one set of exponents to another. In numerical experiments we have found the relative sensitivities to be applicable when there are 10% changes (larger changes were not tried) in NO_x and VOC_R (Kleinman et al., 1997). Eq. (10) has also been tested by doing a sensitivity study on the effects of H_2O on photochemistry in Phoenix. In that test the H_2O concentration was tripled which on average more than doubled the rate of radical production. Fig. 4 compares the $P(O_3)$ increase , $\Delta P(O_3)$, calculated with the CSS model with the corresponding quantity determined from the base case calculation and the change in Q according to:

$$P(O_3)_{3\times H_2O} = P(O_3)_{base} \times (Q_{3\times H_2O}/Q_{base})^{C1}. \quad (20)$$

Even though the change in Q is not a small perturbation, the slope of the regression line indicates semi-quantitative agreement; a bias in $\Delta P(O_3)$ of 16%.

6.1. Relation to closure studies

In a closure experiment one has an over-determined system such that calculated values of $P(O_3)$ can be compared against observations. Given observed values for the variables appearing in the low and high NO_x $P(O_3)$ formulas, (3) and (4), a closure test could be performed. Because K has not been determined, the mid-NO_x formulas cannot be similarly compared. Eq. (10), instead, is a statement about the functional form of lower tropospheric photochemical mechanisms. The functional form is not affected by the circumstance that our measurements are incomplete and that there are additional sources of radicals and VOC reactivity that we are not able to measure. As we have demonstrated that (10) is applicable over a wide range of Q, NO_x, and VOC_R, incomplete measurements merely change these parameters to other values for which (10) applies equally well. Nor is the validity of (10) affected by moderate size changes in rate constants. There are, however, conceivable structural changes to photochemical mechanisms that would invalidate (10). For example, a large radical-aerosol sink, if included in the CSS calculation would cause (10) to predict the wrong functional form for $P(O_3)$. Upper tropospheric chemistry with a large role for HO_2NO_2 as a radical sink (Jaeglé et al., 2001) would likewise lead to an erroneous prediction from (10).

6.2. Extensions

In order to apply (10) one first needs to know L_N/Q. In our case, L_N/Q comes from model output. To a reasonable degree of accuracy, L_N/Q could instead be determined from the approximate equations, (17)–(19). Low and high NO_x regimes where L_N/Q approaches 0 or 1 and $P(O_3)$ is given by (3) and (4), respectively, can usually be identified based only on NO_x concentration. It is possible that with a limited set of measurements 2 or 3 additional L_N/Q categories could be distinguished. This will be easier to do in some locations than in others. For example Fig. 2 shows a near monotonic relation between L_N/Q in Phoenix but considerable scatter in Houston.

An alternate way of using (10) would be to rely totally on concentration fields generated from a time dependent Lagrangian or Eulerian model. In that case model output would be used to determine NO_x concentration, VOC reactivity, radical production rate, L_N/Q, and

$P(O_3)$. An example of such a calculation is given by Spirig et al. (2002), in which a Lagrangian model was used to calculate $P(O_3)$ sensitivities over a larger spatial domain than that covered by surface measurement sites. With model output in hand, Eq. (10) could be used to categorize variations in $P(O_3)$

7. Conclusions

An analytic formula has been derived that shows that $P(O_3)$ is proportional to $Q^{C1}[NO_x]^{C2}$ $(VOC_R)^{C3}$, where Q is a radical production rate, $[NO_x]$ is either NO or NO_2 concentration, VOC_R is the sum total reactivity of all VOCs with OH radical, and the exponents, $C1$, $C2$, and $C3$ depend only on L_N/Q, which is the fraction of free radicals removed from the atmosphere by reacting with NO_x. Aside from an undetermined proportionality constant, the power law formula reduces to previously derived results for low and high NO_x conditions. It shows that there is a smooth transition in behavior in the mid-NO_x regime between the two limiting cases.

Using data that we have accumulated in 5 field programs conducted in Nashville, New York City, Phoenix, Philadelphia, and Houston, we show that the power law expression in most cases quantitatively reproduces the functional form of $P(O_3)$ as predicted from a constrained steady state (CSS) box model. Our analysis shows that the power law formula and CSS model are consistent but does not establish the accuracy of our formula because that depends on the accuracy and completeness of the CSS calculations. One item that we know is missing is the effect of NO_x reservoir compounds such as PAN. We therefore expect our formula to be most accurate in conditions where PAN concentrations are low or where PAN is in steady state. Even with a sizable PAN concentration we have reason to believe that $P(O_3)$ sensitivities and the power law formula for $P(O_3)$ are qualitatively useful.

Just as low and high NO_x formulas for $P(O_3)$ have been helpful in analyzing field data and understanding day to day and place to place variability in $P(O_3)$, we hope that the power law expression will have a similar function in the more general mid-NO_x range. Application of the general formula to mid-NO_x conditions is, however, more demanding as a value for L_N/Q is needed. An analysis of model output, rather than measurements, would naturally yield L_N/Q. The power law formula could then be applied to the task of understanding how and why $P(O_3)$ varies over the model domain.

Acknowledgements

It is a pleasure to acknowledge the contributions of many colleagues who have participated in the 5 field programs used in this study. Colleagues who were there for all or most of the campaigns are Peter Daum, Yin-Nan Lee, Linda Nunnermacker, Stephen Springston, and Judy Weinstein-Lloyd. We thank chief pilot R. Hannigan and the flight crew from PNNL for a job well done. We gratefully acknowledge the Atmospheric Chemistry Program within the Office of Biological and Environmental Research of DOE for supporting field and analysis activities and for providing the G-1 aircraft. This research was performed under sponsorship of the US DOE under contracts DE-AC02-98CH10886.

Appendix A: $\mathrm{dln}\,P(O_3)/\mathrm{dln}\,Q$

Eq. (9) for $\mathrm{dln}\,P(O_3)/\mathrm{dln}\,Q$ is derived following the same procedures used to determine $\mathrm{dln}\,P(O_3)/\mathrm{dln}[NO]$ and $\mathrm{dln}\,P(O_3)/\mathrm{dln}(VOC_R)$ (Kleinman, et al., 1997). Ozone production occurs by the reaction of peroxy radicals with NO in R5–R7 followed by photolysis of NO_2, in R8. The O_3 production rate can therefore be expressed as

$$P(O_3) = k_t([HO_2] + [RO_2])[NO], \quad (A.1)$$

where k_t is a weighted average rate constant for R5–R7. The production rate for radicals (odd hydrogen = $OH + HO_2 + RO_2$), Q, must equal the sum of radical sinks:

$$Q = 2k_{12}[HO_2]^2 + 2k_{13}[HO_2][RO_2] + L_R + L_N, \quad (A.2)$$

where k_{12} is pressure and water vapor concentration dependent. The first 2 terms in (A.2) represent loss of radicals due to production of H_2O_2 and organic peroxides. L_R represents all other radical–radical reactions including $OH + HO_2$ and $RO_2 + R'O_2$, as well as first order loss processes. L_N includes all radical loss reactions between free radicals and NO or NO_2 (R9)–(R11). Eq. (A.2) can be re-arranged to give the total peroxy radical concentration:

$$[HO_2] + [RO_2] = (Q - L_R - L_N)^{1/2}/(2k_{eff})^{1/2}, \quad (A.3)$$

where k_{eff} is an effective rate constant for peroxide formation,

$$k_{eff} = k_{12}(1-a)^2 + k_{13}(1-\alpha)\alpha, \quad (A.4)$$

$$\alpha = [RO_2]/([HO_2] + [RO_2]).$$

Note that $\alpha = 1-\gamma$ in (18) and (19). Distinct symbols are used to maintain consistency with previous publications. Substituting (A.3) into (A.1) gives

$$P(O_3) = k_t/(2k_{eff})^{1/2}(Q - L_R - L_N)^{1/2}[NO]. \quad (A.5)$$

At this point we make our first significant approximation by setting L_R equal to zero. A relative sensitivity of $P(O_3)$ to Q (i.e., $\mathrm{dln}\,P/\mathrm{dln}\,Q = (Q/P)\mathrm{d}P/\mathrm{d}Q$) is

obtained by differentiating (A.5) with respect to Q.

$$\mathrm{d}\ln P(\mathrm{O_3})/\mathrm{d}\ln Q = 1/2Q(1 - \mathrm{d}L_\mathrm{N}/\mathrm{d}Q)/(Q - L_\mathrm{N}). \quad (A.6)$$

A more serious approximation is now made by ignoring organic nitrate and PAN formation leaving just HNO_3 production to contribute to L_N:

$$L_\mathrm{N} \approx P(\mathrm{HNO_3}) = k_9[\mathrm{OH}][\mathrm{NO_2}]. \quad (A.7)$$

The OH concentration appearing in (A.7) is removed from our equations in favor of $P(O_3)$ by expressing $P(O_3)$ as

$$P(\mathrm{O_3}) \approx \Sigma Y_i k_i[\mathrm{OH}][\mathrm{VOC}_i]. \quad (A.8)$$

Eq. (A.8) is an approximation which becomes exact if all peroxy radicals formed from reactions of OH with VOCs go on to react with NO forming O_3. (Tonnesen and Dennis (2000a), Fig. 1d) present results that address part of (A.8), namely the fraction of HO_2 that reacts with NO. Except at low NO_x concentration that fraction is 80–100%, sufficiently close to unity that (A.8) is a useable approximation. However, at low NO_x the primary fate of a peroxy radical is to form peroxides. That (A.8) is no longer valid at low NO_x has very little effect on our final results as under that condition L_N and its derivatives are close to zero.

Substituting (A.7) into (A.8) yields,

$$L_\mathrm{N} = (k_9[\mathrm{NO_2}]/\Sigma Y_i k_i[\mathrm{VOC}_i])\, P(\mathrm{O_3}). \quad (A.9)$$

Eq. (A.9) is differentiated with respect to Q, yielding

$$\mathrm{d}L_\mathrm{N}/\mathrm{d}Q = (L_\mathrm{N}/Q)\,\mathrm{d}\ln P(\mathrm{O_3})/\mathrm{d}\ln Q \quad (A.10)$$

which is substituted into (A.6). After collecting like terms we obtain

$$\mathrm{d}\ln P(\mathrm{O_3})/\mathrm{d}\ln Q = (1/2)/(1 - 1/2\,L_\mathrm{N}/Q). \quad (A.11)$$

References

Atkinson, R., 2000. Atmospheric chemistry of VOCs and NO_x. Atmospheric Environment 34, 2063–2101.

Cantrell, C.A., Shetter, R.E., Gilpin, T.M., Calvert, J.G., Eisele, F.L., Tanner, D.J., 1996. Peroxy radical concentrations measured and calculated from trace gas measurements in the Mauna Loa Observatory Photochemistry Experiment 2. Journal of Geophysical Research 101, 14653–14664.

Cantrell, C.A., et al., 2003. Steady state free radical budgets and ozone photochemistry during TOPSE. Journal of Geophysical Research 108 (D4).

Carmichael, G.R., et al., 2003. Regional-scale chemical transport modeling in support of the analysis of observations obtained during the TRACE-P experiment. Journal of Geophysical Research 108 (D21).

Carpenter, L.J., Monks, P.S., Bandy, B.J., Penkett, S.A., Galbally, I.E., Meyer, C.P., 1997. A study of peroxy radicals and ozone photochemistry at coastal sites in the northern and southern hemispheres. Journal of Geophysical Research 102, 25417–25427.

Carpenter, L.J., Green, T.J., Mills, G.P., Bauguitte, S., Penkett, S.A., Zanis, P., Schuepbach, E., Schmidbauer, N., Monks, P.S., Zellweger, C., 2000. Oxidized nitrogen and ozone production efficiencies in the springtime free troposphere over the Alps. Journal of Geophysical Research 105, 14547–14559.

Daum, P.H., Kleinman, L.I., Imre, D., Nunnermacker, L.J., Lee, Y.-N., Springston, S.R., Newman, L., Weinstein-Lloyd, J., Valente, R.J., Imhoff, R.E., Tanner, R.L., Meagher, J.F., 2000a. Analysis of O_3 formation during a stagnation episode in Central TN in Summer 1995. Journal of Geophysical Research 105, 9107–9120.

Daum, P.H., Kleinman, L., Imre, D.G., Nunnermacker, L.J., Lee, Y.-N., Springston, S.R., Newman, L., 2000b. Analysis of the processing of Nashville urban emissions on July 3 and July 18, 1995. Journal of Geophysical Research 105, 9155–9164.

Daum, P.H., Kleinman, L.I., Springston, S.R., Nunnermacker, L.J., Lee, Y.-N., Weinstein-Lloyd, J., Zheng, J., Berkowitz, C., 2003. A comparative study of O_3 formation in the Houston urban and industrial plumes during the TEXAQS 2000 Study. Journal of Geophysical Research 108 (D23), 4715.

Dommen, J., Prévôt, A.S.H., Neininger, B., Bäumle, M., 2002. Characterization of the photooxidant formation in the metropolitan area of Milan from aircraft measurements. Journal of Geophysical Research 107 (D22).

Field, R.J., Hess, P.G., Kalachev, L.V., Madronich, S., 2001. Characterization of oscillation and a period-doubling transition to chaos reflecting dynamic instability in a simplified model of tropospheric chemistry. Journal of Geophysical Research 102, 7553–7565.

Frost, G.J., et al., 1998. Photochemical ozone production in the rural southeastern United States during the 1990 ROSE program. Journal of Geophysical Research 103, 22491–22508.

Hammer, M.-U., Vogel, B., Vogel, H., 2002. Findings on H_2O_2/HNO_3 as an indicator of ozone sensitivity in Baden-Württemberg, Berlin-Brandenburg, and the Po valley based on numerical simulations. Journal of Geophysical Research 107 (D22).

Jacob, D.J., Heikes, B.J., Fan, S.-M., Logan, J.A., Mauzerall, D.L., Bradshaw, J.D., Singh, H.B., Gregory, G.L., Talbot, R.W., Blake, D.R., Sachse, G.W., 1996. Origin of ozone and NO_x in the tropical troposphere: A photochemical analysis of aircraft observations over the South Atlantic basin. Journal of Geophysical Research 101, 24235–24250.

Jaeglé, L., Jacob, D.J., Brune, W.H., Wennberg, P.O., 2001. Chemistry of HO_x radicals in the upper troposphere. Atmospheric Environment 35, 469–489.

Kleinman, L.I., Lee, Y.-N., Springston, S.R., Nunnermacker, L., Zhou, X., Brown, R., Hallock, K., Klotz, P., Leahy, D., Lee, J.H., Newman, L., 1994. Ozone formation at a rural site in the southeastern US. Journal of Geophysical Research 99, 3469–3482.

Kleinman, L.I., Daum, P.H., Lee, J.H., Lee, Y.-N., Nunnermacker, L.J., Springston, S.R., Newman, L., Weinstein-Lloyd, J., Sillman, S., 1997. Dependence of ozone

production on NO and hydrocarbons in the troposphere. Geophysical Research Letters 24, 2299–2302.

Kleinman, L.I., Daum, P.H., Lee, Y.-N., Nunnermacker, L.J., Springston, S.R., Weinstein-Lloyd, J., Rudolph, J., 2001. Sensitivity of ozone production rate to ozone precursors. Geophysical Research Letters 28, 2903–2906.

Kleinman, L.I., Daum, P.H., Imre, D., Lee, Y.-N., Nunnermacker, L.J., Springston, S.R., Weinstein-Lloyd, J., Rudolph, J., 2002a. Ozone production rate and hydrocarbon reactivity in 5 urban areas: a cause of high ozone concentration in Houston. Geophysical Research Letters 29 (10).

Kleinman, L.I., Daum, P.H., Lee, Y.-N., Nunnermacker, L.J., Springston, S.R., Weinstein-Lloyd, J., Rudolph, J., 2002b. Ozone production efficiency in an urban area. Journal of Geophysical Research 107 (D23).

Liu, S.C., Trainer, M., Carroll, M.A., Hübler, G., Montzka, D.D., Norton, R.B., Ridley, B.A., Walega, J.G., Atlas, E.L., Heikes, B.G., Huebert, B.J., Warren, W., 1992. A study of the photochemistry and ozone budget during the Mauna Loa Observatory Photochemistry Experiment. Journal of Geophysical Research 97, 10463–10471.

Madronich,, S., 1987. Photodissociation in the atmosphere 1. Actinic flux and the effects of ground reflections and clouds. Journal of Geophysical Research 92, 9740–9752.

Martilli, A., Neftel, A., Favaro, G., Kirchner, F., Sillman, S., Clappier, A., 2002. Simulation of the ozone formation in the northern part of the Po Valley. Journal of Geophysical Research 107 (D22).

Mihelcic, D., et al., 2003. Peroxy radicals during BERILOZ at Pabstthum: Measurements, radical budgets and ozone production. Journal of Geophysical Research 108 (D4).

Paulson, S.E., Seinfeld, J.H., 1992. Development and evaluation of a photochemical mechanism for isoprene. Journal of Geophysical Research 97, 20703–20715.

Penkett, S.A., Clemitshaw, K.C., Savage, N.H., Burgess, R.A., Cardenas, L.M., McFadyen, G.G., Cape, J.N., 1999. Studies of oxidant production at the Weybourne Atmospheric Observatory in summer and winter conditions. Journal of Atmospheric Chemistry 33, 111–128.

Ridley, B.A., Madronich, S., Chatfield, R.B., Walega, J.G., Shetter, R.E., Carroll, M.A., Montzka, D.D., 1992. Measurements and model simulations of the photostationary state during the Mauna Loa Observatory Photochemistry Experiment: Implications for radical concentrations and ozone production and loss rates. Journal of Geophysical Research 97, 10,375–10,388.

Seinfeld, J.H., Pandis, S.N., 1997. Atmospheric Chemistry and Physics—From Air Pollution to Climate Change. Wiley-Interscience, New York.

Sillman, S., 1995. The use of NO_y, HCHO, H_2O_2 and HNO_3 as indicators for ozone-NO_x-hydrocarbon sensitivity in urban locations. Journal of Geophysical Research 100, 14175–14188.

Sillman, S., He, D., 2002. Some theoretical results concerning O3-NO_x-VOC chemistry and NO_x-VOC indicators. Journal of Geophysical Research 107 (D22).

Spirig, C., Neftel, A., Kleinman, L., Hjorth, J., 2002. NO_x versus VOC limitation to O3 production in the Po valley: local and integrated view based on observations. Journal of Geophysical Research 107 (D22).

Stewart, R.W., 1995. Dynamics of the low to high NO_x transition in a simplified tropospheric photochemical model. Journal of Geophysical Research 101, 8929–8943.

Stockwell, W.R., Middleton, P., Chang, J.S., Tang, X., 1990. The second generation regional acid deposition model chemical mechanism for regional air quality modeling. Journal of Geophysical Research 95, 16343–16367.

Thielmann, A., Prévôt, A.S.H., Staehelin, J., 2002. Sensitivity of ozone production derived from field measurements in the Italian Po basin. Journal of Geophysical Research 107 (D22).

Thornton, J.A., Wooldridge, P.J., Cohen, R.C., Martinez, M., Harder, H., Brune, W.H., Williams, E.J., Roberts, J.M., Fehsenfeld, F.C., Hall, S.R., Shetter, R.E., Wert, B.P., Fried, A., 2002. Ozone production rate as a function of NO_x abundances and HO_x production rates in the Nashville urban plume. Journal of Geophysical Research 107 (D12).

Tonnesen, G.S., Dennis, R.L., 2000a. Analysis of radical propagation efficiency to assess ozone sensitivity to hydrocarbons and NO_x 1. Local indicators of instantaneous odd oxygen production sensitivity. Journal of Geophysical Research 105, 9213–9225.

Tonnesen, G.S., Dennis, R.L., 2000b. Analysis of radical propagation efficiency to assess ozone sensitivity to hydrocarbons and NO_x 2. Long-lived species as indicators of ozone concentration sensitivity. Journal of Geophysical Research 105, 9227–9241.

Volz-Thomas, A., Pätz, H.-W., Houben, N., Konrad, K., Klüpfel, T., Perner, D., 2003. Inorganic trace gases and peroxy radicals during BERLIOZ at Pabstthum: an investigation of the photostationary state of NO_x and O_3. Journal of Geophysical Research 108 (D4).